TECHNISCHE UNIVERSITÄT WIEN
Vienna University of Technology

Operations Research and Control Systems

# Environmental Regulations, Abatement and Economic Growth

*Elke Moser, Alexia Prskawetz, Gernot Tragler*

**Research Report 2011-02**

March, 2011

**Operations Research and Control Systems**
Institute of Mathematical Methods in Economics
Vienna University of Technology

Research Unit ORCOS
Argentinierstraße 8/E105-4,
1040 Vienna, Austria
E-mail: orcos@eos.tuwien.ac.at

# Environmental Regulations, Abatement and Economic Growth

Elke Moser*, Alexia Prskawetz†, Gernot Tragler‡

**Abstract**

Due to recent global discussions about climate change and its possible consequences, the usage of environmental policy instruments with the intent to counteract against the current environmental developments has become increasingly important. Environmental regulation as policy instrument is supposed to reduce or ideally minimize emissions and pollution. However, the question arises how effective such regulations really are. Further on it is not obvious whether they rather repress innovation and economic growth than induce a shift towards a greener technology. To address these questions we investigate an endogenous growth model in an environmental context, introduced by M.Rauscher [Green R & D versus End-of-Pipe Emission Abatement: A Model of Directed Technical Change. Thuenen-Series of Applied Economic Theory, 106, 2009]. There, the author investigates the impact of environmental standards on capital accumulation and R&D investments in an economy where both, brown (dirty) as well as green (clean) capital can be used in production. While Rauscher keeps the problem formulation rather general without assuming specific model functions, our focus is to apply optimal control theory to a specific scenario of this model.

*Vienna Institute of Demography, Austrian Academy of Sciences, Wohllebengasse 12-14, 1040 Vienna, Austria (elke.moser@oeaw.ac.at)

†Institute of Mathematical Methods in Economics, Research Group Economics, Vienna University of Technology, Argentinierstrasse 8, 1040 Vienna (afp@econ.tuwien.ac.at), and Vienna Institute of Demography, Wohllebengasse 12-14, 1040 Vienna, Austria

‡Institute of Mathematical Methods in Economics, Research Group ORCOS, Vienna University of Technology, Argentinierstrasse 8, 1040 Vienna (gernot.tragler@tuwien.ac.at)

# 1 Introduction

In recent years climate change and the possible consequences that human society might have to deal with, if further global warming cannot be stopped, have become one of the most important topics in science, politics and the world wide media. The scientific evidence that many key climate indicators are already moving beyond the patterns of natural variability defines this dramatic change as a world wide concern. Hence, the importance of climate mitigation has become undeniable. These indicators, including global mean surface temperature, global ocean temperature, global average sea level, northern hemisphere snow cover and Arctic sea ice decline as well as extreme climatic events, additionally come along with the risk of abrupt or irreversible climatic shifts, which might have devastating consequences for the entire world population. This underlines how urgent the need of climate actions has become (see Richardson et al. [2009]).

In the 4th Assessment Report by the International Panel on Climate Change (IPCC [2007]), scientific evidence on global warming, its damages and the importance of climate mitigation as well as the reduction of anthropogenic greenhouse gas (GHG) emissions are demonstrated extensively. According to their *Synthesis Report*, the industry sector, besides the energy supply and transport sectors is one of the main sources of anthropogenic GHG emissions with a portion of almost 20% (2004). The majority are $CO_2$ emissions due to the use of fossil fuels, but also the emissions of other gases like $PFCs$, $SF_6$, $CH_4$ and $N_2O$ due to physical and chemical processes yield an essential fraction. Additionally, one has to consider the polluting impact of industrial waste and wastewater. Further on, not only the sources are discussed in IPCC [2007] but also a broad range of mitigation policy measures are suggested, which especially emphasizes the role of technology policies and the increasing need for more R&D efforts. In the *Mitigation of Climate Change Report*, some possible mitigation options for a greener technology are explained, such as fuel switching, including the use of waste material, advanced energy efficiency, the use of bioenergy and material recycling and substitution. As far as according policy instruments are concerned, they consider performance standards, subsidies, tax credits, tradeable permits and voluntary agreements as the most environmentally effective ones.

Although these environmental policy instruments seem to be promising, the question arises how they can be utilized in the most effective way and whether strict environmental regulation has a supporting or repressing impact on innovation and economic growth. To answer these questions we refer to a recent paper by Rauscher [2009] who already addressed this issue in his paper by constructing a simple dynamic environmental-economic model which considers capital accumulation, end-of-pipe emission abatement, R&D investments and knowledge spillovers in an endogenous growth framework. He investigates in a conveniently tractable way whether tighter environmental standards will induce a shift from end-of-pipe emission abatement to a process-integrated one and which impact they have on R&D investments and growth. The model Rauscher employs is kept algebraically simple without specifying concrete functional forms. In this paper we introduce specific functional forms and apply optimal control theory to solve for the dynamic paths of the environmental-economic system.

The paper is organized as follows. In the next section we introduce the model, which is solved in section third applying Pontryagin's Maximum Principle. Numerical simulations, including a bifurcation analysis, are presented in the fourth section. Section five concludes and gives an outlook for further research.

## 2 The Model

To investigate the effects of environmental standards on economic growth and R&D investments, we build on the model originally worked out by Rauscher [2009], who considers a competitive market economy where a continuum of identical firms using identical technologies produce a homogenous GDP good. In this economy two types of capital are accumulated: first, there is *conventional capital*, also called *brown capital*, which is pollutive and therefore not quite eco-friendly, secondly, non-polluting *green capital* can be chosen. Additionally, the government sets environmental standards which the entrepreneurs are obligated to meet. The necessary abatement effort as well as the abatement costs depend on the stringency of these regulations. Consequently, firms adopting cleaner technologies have to spend less on end-of-pipe abatement. This benefit, however, comes at a cost because the required resources for green R&D could be invested otherwise profitably in conventional R&D. Instead of assuming different groups of agents, as frequently done in many other papers approaching this topic, Rauscher [2009] focuses on one type of agent in the private sector of the economy, who is a capital-owning entrepreneur doing his/her R&D in-house and who saves and consumes all at the same time. In case of perfect competition of the markets on which these agents interact, the simple homogenous-representative-agent model generates the same results as its more elaborated version with heterogeneous agents.

Maximizing his/her own profit, this representative agent has to consider the present value of future utility, given as

$$\int_0^\infty e^{-rt}(\ln(C(t)) + u(\varepsilon))dt \quad \text{with} \quad C(t) > 0, \tag{1}$$

where $C(t)$ is the consumption or dividend income, $\ln(C(t))$ describes the utility level that one can get out of it and $r$ is the discount rate. Further on, $\varepsilon$ specifies the environmental quality determined by the government due to their required standards. It is considered as exogenously given and is an index between 0 and 1, where $\varepsilon = 0$ denotes the laissez-faire scenario describing an economy without any environmental regulation and therefore with bad environmental quality. On the other side, the maximal attainable environmental quality is given at $\varepsilon = 1$, where no pollution exists at all. The private sector's utility of environmental quality is denoted as $u(\varepsilon)$ and will be set in the following as $u(\varepsilon) = c\varepsilon^\gamma$ with $c > 0$ and $0 < \gamma < 1$.

The entrepreneurs use conventional capital $K(t)$ and/or green capital $G(t)$ to produce an output

$$\begin{gathered} F(K(t), G(t)) = bK(t)^{\alpha_1} G(t)^{\alpha_2} \\ \text{with } b > 0,\ t \in [0, \infty),\ 0 < \alpha_2 \leq \alpha_1 < 1 \text{ and } \alpha_1 + \alpha_2 \leq 1. \end{gathered} \tag{2}$$

One of the central assumptions in this model is that the output is used completely for consumption, for the coverage of opportunity costs due to R&D investments of either type and for end-of-pipe emission

abatement, which is summarized in the following budget constraint:

$$F(K(t),G(t)) - C(t) - w(R_K(t) + R_G(t)) - \chi(\varepsilon)K(t) = 0. \tag{3}$$

Note that as of here, we will often omit the time argument $t$ for the ease of exposition. $R_K$ and $R_G$ denote the investments for R&D to generate new capital of types $K$ and $G$, respectively. The parameter $w \in [0,1]$ represents the exogenous opportunity costs. The abatement costs for achieving the binding environment constraints of the government are proportional to the installed conventional capital $K$. The costs per unit capital is given as $\chi(\varepsilon)$ which is increasing and convex in the stringency of environmental regulation, i.e. $\chi' > 0, \chi'' > 0$, and will be set for this analysis as $\chi(\varepsilon) = a\varepsilon^{\beta}$ with $a > 0$ and $\beta > 1$.

Regarding the state dynamics for the two types of capital, we use a Cobb Douglas production function with decreasing returns to scale:

$$\dot{K} = A(K,R_K) = dK^{\delta_1}{R_K}^{\delta_2} - \phi K \quad \text{with} \quad \delta_1 + \delta_2 < 1, \tag{4}$$

$$\dot{G} = B(G,R_G) = eG^{\sigma_1}{R_G}^{\sigma_2} - \psi G \quad \text{with} \quad \sigma_1 + \sigma_2 < 1. \tag{5}$$

The existing capital stock itself has a positive feedback on the accumulation. Assuming that this positive feedback is weaker than the contribution of new technology due to R&D, the partial elasticity of production of the capital stock is supposed to be less than the one of the R&D investments. Hence, $\delta_1 < \delta_2$ and $\sigma_1 < \sigma_2$. Additionally, it is more likely that conventional capital is more established in the economy than green one and therefore accumulation is much easier. To take this imbalance into account, the partial elasticities of green capital $G$ should at least not be greater than those of conventional capital $K$, i.e. $\sigma_1 \leq \delta_1$ and $\sigma_2 \leq \delta_2$. Further on, one has to consider that capital of either type is subject to depreciation over time due to wear and tear as well as obsolescence. Therefore, also depreciation rates $\phi$ and $\psi$ are included.

Figure 1 shows the interrelations of the described variables to illustrate the dynamics of the model. Starting from the capital stocks $K$ and $G$, output $F(K,G)$ is produced. Constraint by the available budget (3), the decision-maker has to determine the extend of R&D investments that are made for either brown ($R_K$) or green ($R_G$) capital or possibly both investments. These investments in turn influence the growth of the capital stocks $K$ and $G$, respectively. Additionally, also the existing capital stock contributes to the accumulation .

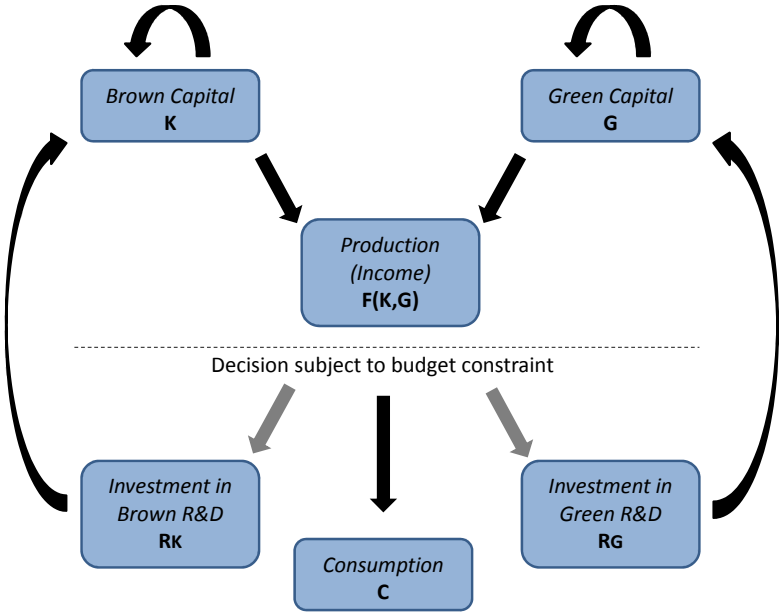


Figure 1: Sketch of the dynamics of the model.

Solving equation (3) for consumption $C$ together with (1) leads to an optimal control problem with $R_K$ and $R_G$ as control variables and the two available types of capital as states, which is given as

$$\max_{R_K,R_G} \int_0^\infty e^{-rt}\left(\ln\left(bK^{\alpha_1}G^{\alpha_2} - w(R_K+R_G) - a\varepsilon^\beta K\right) + c\varepsilon^\gamma\right)dt \tag{6}$$

$$\begin{aligned}
\text{s.t.:}\quad & \dot{K} = dK^{\delta_1}R_K^{\delta_2} - \phi K && \text{(6a)}\\
& \dot{G} = eG^{\sigma_1}R_G^{\sigma_2} - \psi G && \text{(6b)}\\
& 0 \le R_K \quad \forall t \ge 0 && \text{(6c)}\\
& 0 \le R_G \quad \forall t \ge 0 && \text{(6d)}\\
& 0 < bK^{\alpha_1}G^{\alpha_2} - w(R_K+R_G) - a\varepsilon^\beta K && \text{(6e)}\\
& 0 \le \varepsilon \le 1 && \text{(6f)}\\
& 0 < \alpha_1, \alpha_2, \gamma, w < 1 \quad \text{and} \quad \alpha_1+\alpha_2 \le 1 && \text{(6g)}\\
& 0 < \delta_1, \delta_2 < 1 \quad \text{and} \quad \delta_1+\delta_2 < 1 && \text{(6h)}\\
& 0 < \sigma_1, \sigma_2 < 1 \quad \text{and} \quad \sigma_1+\sigma_2 < 1 && \text{(6i)}\\
& 1 < \beta && \text{(6j)}\\
& 0 < \phi, \psi, a, b, c, d, e, r. && \text{(6k)}
\end{aligned}$$

# 3 Analytical results

## 3.1 Derivation of the Canonical System

Summing up, we consider a discounted autonomous model with infinite planning horizon. To derive the necessary conditions for an optimal solution we consider the Lagrangian $\mathcal{L}$ in current value notation, where $\mathcal{H}$ denotes the Hamiltonian, $\mathcal{C}$ the control and mixed path constraints and $\mu$ the vector of Lagrange Multipliers:

$$\begin{aligned}\mathcal{L} = \mathcal{H} + \mu\mathcal{C} &= \lambda_0(\ln(F(K,G) - w(R_K + R_G) - \chi(\varepsilon)K) + u(\varepsilon)) + \\ &\quad \lambda_1 A(K,R_K) + \lambda_2 B(G,R_G) + \mu_1 R_K + \mu_2 R_G + \\ &\quad \mu_3(F(K,G) - w(R_K + R_G) - \chi(\varepsilon)K)\end{aligned}$$

with the co-states $(\lambda_0, \lambda_1, \lambda_2) \neq 0$. Then the first order conditions are

$$\mathcal{L}_{R_K} = \frac{-w\lambda_0}{F(K,G) - w(R_K + R_G) - \chi(\varepsilon)K} + \lambda_1 A_{R_K} + \mu_1 - w\mu_3 = 0 \tag{7}$$

$$\mathcal{L}_{R_G} = \frac{-w\lambda_0}{F(K,G) - w(R_K + R_G) - \chi(\varepsilon)K} + \lambda_2 B_{R_G} + \mu_2 - w\mu_3 = 0 \tag{8}$$

$$\dot{\lambda_1} = \lambda_1(r - A_K) - \lambda_0 \frac{F_K(K,G) - \chi(\varepsilon)}{F(K,G) - w(R_K + R_G) - \chi(\varepsilon)K} - \mu_3(F_K(K,G) - \chi(\varepsilon)) \tag{9}$$

$$\dot{\lambda_2} = \lambda_2(r - B_G) - \lambda_0 \frac{F_G(K,G)}{F(K,G) - w(R_K + R_G) - \chi(\varepsilon)K} - \mu_3 F_G(K,G) \tag{10}$$

where subscripts denote partial derivatives of multivariate functions. The complementary slackness conditions are

$$\begin{aligned}\mu_1 &\geq 0 \quad \text{and} \quad 0 = \mu_1 R_K \\ \mu_2 &\geq 0 \quad \text{and} \quad 0 = \mu_2 R_G \\ \mu_3 &\geq 0 \quad \text{and} \quad 0 = \mu_3(F(K,G) - w(R_K + R_G) - \chi(\varepsilon)K).\end{aligned} \tag{11}$$

One can show that $\lambda_0 = 1$, without loss of generality. For the derivation of the canonical system one has to distinguish between the different cases of an interior arc and a boundary arc. In the first case none of the constraints are active and, due to the complementary slackness conditions in 11, $(\mu_1, \mu_2, \mu_3) = 0$. Hence, an optimal control should maximize the current value Hamiltonian, i.e.

$$({R_K}^*, {R_G}^*) = \arg\max_{(R_K, R_G)} \mathcal{H}$$

and therefore

$$\mathcal{L}_{R_K} = \mathcal{H}_{R_K} = 0 \tag{12}$$

$$\mathcal{L}_{R_G} = \mathcal{H}_{R_G} = 0 \quad . \tag{13}$$

To prove that the Hamiltonian is strict concave, the positivity of the co-states is necessary which can be shown by solving (12) and (13) for $\lambda_1$ and $\lambda_2$ respectively. This yields

$$\begin{aligned}\lambda_1 &= \frac{w}{(F(K,G)-w(R_K+R_G)-a\varepsilon^\beta K)A_{R_K}(K,R_K)} > 0\\ \lambda_2 &= \frac{w}{(F(K,G)-w(R_K+R_G)-a\varepsilon^\beta K)B_{R_G}(G,R_G)} > 0.\end{aligned}$$

Note that $A_{R_KR_K}(K,R_K) < 0$ and $B_{R_GR_G}(G,R_G) < 0$. The Hessian matrix of the Hamiltonian

$$H = \begin{pmatrix} -\frac{w^2}{(F(K,G)-w(R_K+R_G)-\chi(\varepsilon)K)^2} + \lambda_1 A_{R_KR_K}(K,R_K) & -\frac{w^2}{(F(K,G)-w(R_K+R_G)-\chi(\varepsilon)K)^2} \\ -\frac{w^2}{(F(K,G)-w(R_K+R_G)-\chi(\varepsilon)K)^2} & -\frac{w^2}{(F(K,G)-w(R_K+R_G)-\chi(\varepsilon)K)^2} + \lambda_2 B_{R_GR_G}(G,R_G) \end{pmatrix}$$

therefore is negative definite and the Hamiltonian $\mathcal{H}$ is strict concave.

The optimality conditions in (12) and (13) allow to derive control functions depending on co-state and state variables (cf. conditions (7) and (8))

$$\begin{aligned}R_K &= R_K(K,G,\lambda_1,\lambda_2)\\ R_G &= R_G(K,G,\lambda_1,\lambda_2).\end{aligned} \tag{14}$$

Substituting these control functions into the state dynamics (4) and (5) as well as into the adjoint equations (9) and (10) the canonical system in the state-co-state-space is given as

$$\begin{aligned}\dot{K} &= A(K,R_K(K,G,\lambda_1,\lambda_2))\\ \dot{G} &= B(G,R_G(K,G,\lambda_1,\lambda_2))\\ \dot{\lambda_1} &= \lambda_1(r-A_K) - \frac{F_K(K,G)-\chi(\varepsilon)}{F(K,G)-w(R_K(K,G,\lambda_1,\lambda_2)+R_G(K,G,\lambda_1,\lambda_2))-\chi(\varepsilon)K}\\ \dot{\lambda_2} &= \lambda_2(r-B_G) - \frac{F_G(K,G)}{F(K,G)-w(R_K(K,G,\lambda_1,\lambda_2)+R_G(K,G,\lambda_1,\lambda_2))-\chi(\varepsilon)K}.\end{aligned}$$

However, from an application orientated point of view it is often more convenient to transform the canonical system from the state-co-state-space into the state-control-space. Within this representation immediate interpretation of the results is more convenient (see Grass, Caulkins, Feichtinger, Tragler, and Behrens [2008]). Additionally, inserting the model functions from above, the two controls from (7) and (8) are given only implicitly. Therefore, the derivation of the canonical system in the state-control space is even necessary.

Considering the model functions from above, the first order conditions are

$$\mathcal{H}_{R_K} = -\frac{w}{bK^{\alpha_1}G^{\alpha_2}-w(R_K+R_G)-a\varepsilon^\beta K} + \lambda_1(dK^{\delta_1}\delta_2 {R_K}^{\delta_2-1}) = 0 \tag{15a}$$

$$\mathcal{H}_{R_G} = -\frac{w}{bK^{\alpha_1}G^{\alpha_2}-w(R_K+R_G)-a\varepsilon^\beta K} + \lambda_2(eG^{\sigma_1}\sigma_2 {R_G}^{\sigma_2-1}) = 0 \tag{15b}$$

$$\dot{\lambda_1} = \lambda_1(r-d\delta_1 K^{\delta_1-1}{R_K}^{\delta_2}+\phi) - \frac{\alpha_1 bK^{\alpha_1-1}G^{\alpha_2}-a\varepsilon^\beta}{bK^{\alpha_1}G^{\alpha_2}-w(R_K+R_G)-a\varepsilon^\beta K} \tag{15c}$$

$$\dot{\lambda_2} = \lambda_2(r-e\sigma_1 G^{\sigma_1-1}{R_G}^{\sigma_2}+\psi) - \frac{\alpha_2 bK^{\alpha_1}G^{\alpha_2-1}}{bK^{\alpha_1}G^{\alpha_2}-w(R_K+R_G)-a\varepsilon^\beta K}. \tag{15d}$$

Solving 15a and 15b for $\lambda_1$ and $\lambda_2$ instead of the controls yields

$$\begin{aligned}\lambda_1(K,G,R_K,R_G) &= \frac{w}{(bK^{\alpha_1}G^{\alpha_2}-w(R_K+R_G)-a\varepsilon^{\beta}K)dK^{\delta_1}\delta_2{R_K}^{\delta_2-1}} \\ \lambda_2(K,G,R_K,R_G) &= \frac{w}{(bK^{\alpha_1}G^{\alpha_2}-w(R_K+R_G)-a\varepsilon^{\beta}K)eG^{\sigma_1}\sigma_2{R_G}^{\sigma_2-1}}.\end{aligned} \tag{16}$$

By using the total time derivatives of the co-states

$$\begin{aligned}\dot{\lambda_1} &= \lambda_{1_K}\dot{K}+\lambda_{1_G}\dot{G}+\lambda_{1_{R_K}}\dot{R_K}+\lambda_{1_{R_G}}\dot{R_G} \\ \dot{\lambda_2} &= \lambda_{2_K}\dot{K}+\lambda_{2_G}\dot{G}+\lambda_{2_{R_K}}\dot{R_K}+\lambda_{2_{R_G}}\dot{R_G}\end{aligned} \tag{17}$$

two equations for the control dynamics can be obtained. Together with the adjoint dynamics in (15c) and (15c) these control dynamics are given as

$$\begin{aligned}\dot{R_K} &= -\frac{\dot{\lambda_2}\lambda_{1_{R_G}}-\dot{\lambda_1}\lambda_{2_{R_G}}+\dot{G}(\lambda_{1_G}\lambda_{2_{R_G}}-\lambda_{1_{R_G}}\lambda_{2_G})+\dot{K}(\lambda_{1_K}\lambda_{2_{R_G}}-\lambda_{1_{R_G}}\lambda_{2_K})}{\lambda_{1_{R_K}}\lambda_{2_{R_G}}-\lambda_{1_{R_G}}\lambda_{2_{R_K}}} \\ \dot{R_G} &= -\frac{\dot{\lambda_1}\lambda_{2_{R_K}}-\dot{\lambda_2}\lambda_{1_{R_K}}+\dot{G}(\lambda_{1_{R_K}}\lambda_{2_G}-\lambda_{1_G}\lambda_{2_{R_K}})+\dot{K}(\lambda_{1_{R_K}}\lambda_{2_K}-\lambda_{1_K}\lambda_{2_{R_K}})}{\lambda_{1_{R_K}}\lambda_{2_{R_G}}-\lambda_{1_{R_G}}\lambda_{2_{R_K}}}\end{aligned} \tag{18}$$

which yields the canonical system

$$\begin{aligned}\dot{R_K} &= \frac{{D_1}^2D_2^2{R_G}^2{R_K}^2Y^3}{w^2\left(d(\delta_2-1)\delta_2K^{\delta_1}{R_K}^{\delta_2}\left(D_2{R_G}^2w-eY(\sigma_2-1)\sigma_2G^{\sigma_1}{R_G}^{\sigma_2}\right)+D_1e{R_K}^2w(\sigma_2-1)\sigma_2G^{\sigma_1}{R_G}^{\sigma_2}\right)} \\ &\quad .\left\{\left[\left(eY(\sigma_2-1)\sigma_2G^{\sigma_1}{R_G}^{\sigma_2-2}-D_2w\right)\left(D_1(a\varepsilon^{\beta}-b\alpha_1G^{\alpha_2}K^{\alpha_1-1})+w\left(-d\delta_1K^{\delta_1-1}{R_K}^{\delta_2}+r+\phi\right)\right)+\right.\right. \\ &\quad \left.\left.D_2w\left(w\left(-e\sigma_1G^{\sigma_1-1}{R_G}^{\sigma_2}+r+\psi\right)-bD_2\alpha_2G^{\alpha_2-1}K^{\alpha_2}\right)\right]\frac{w}{D_1{D_2}^2Y^3}+\dot{G}T_1+\dot{K}T_2\right\} \\ \dot{R_G} &= \frac{{D_1}^2D_2^2{R_G}^2{R_K}^2Y^3}{w^2\left(d(\delta_2-1)\delta_2K^{\delta_1}{R_K}^{\delta_2}\left(D_2{R_G}^2w-eY(\sigma_2-1)\sigma_2G^{\sigma_1}{R_G}^{\sigma_2}\right)+D_1e{R_K}^2w(\sigma_2-1)\sigma_2G^{\sigma_1}{R_G}^{\sigma_2}\right)} \\ &\quad .\left\{\left[\left(dY(\delta_2-1)\delta_2K^{\delta_1}{R_K}^{\delta_2-2}-D_1w\right)\left(w\left(-e\sigma_1G^{\sigma_1-1}{R_G}^{\sigma_2}+r+\psi\right)-bD_2\alpha_2G^{\alpha_2-1}K^{\alpha_2}\right)+\right.\right. \\ &\quad \left.\left.D_1w\left(aD_1\varepsilon^{\beta}-bD_1\alpha_1G^{\alpha_2}K^{\alpha_1-1}-dw\delta_1K^{\delta_1-1}{R_K}^{\delta_2}+w(r+\phi)\right)\right]\frac{w}{D_1{D_2}^2Y^3}+\dot{G}T_3+\dot{K}T_4\right\}\end{aligned}$$

$$\begin{aligned}\dot{K} &= dK^{\delta_1}{R_K}^{\delta_2}-\phi K \\ \dot{G} &= eG^{\sigma_1}{R_G}^{\sigma_2}-\psi G\end{aligned} \tag{19}$$

with

$$T_1 = \frac{ew^2\sigma_2G^{\sigma_1-1}{R_G}^{\sigma_2-2}\left(b\alpha_2(\sigma_2-1)G^{\alpha_2}K^{\alpha_1}+R_Gw\sigma_1\right)}{D_1{D_2}^2Y^3}$$

$$\begin{aligned}T_2 &= -\frac{w^2}{{D_1}^2{D_2}^2K{R_G}^2R_KY^3}\left(d\delta_1\delta_2K^{\delta_1}{R_K}^{\delta_2}\left(D_2{R_G}^2w-eY(\sigma_2-1)\sigma_2G^{\sigma_1}{R_G}^{\sigma_2}\right)-\right. \\ &\quad \left.D_1e{R_K}(\sigma_2-1)\sigma_2G^{\sigma_1}{R_G}^{\sigma_2}\left(b\alpha_1G^{\alpha_2}K^{\alpha_1}-aK\varepsilon^{\beta}\right)\right)\end{aligned}$$

$$
\begin{aligned}
T_3 &= \frac{w^2}{{D_1}^2 {D_2}^2 G {R_K}^2 Y^3}\Big(d(\delta_2-1)\delta_2 K^{\delta_1} {R_K}^{\delta_2}\left(bD_2 R_G \alpha_2 G^{\alpha_2} K^{\alpha_1} + eY\sigma_1\sigma_2 G^{\sigma_1} {R_G}^{\sigma_2}\right) - \\
&\quad D_1 e {R_K}^2 w \sigma_1 \sigma_2 G^{\sigma 1} {R_G}^{\sigma_2}\Big) \\
T_4 &= \frac{dw^2\delta_2 K^{\delta_1-1} {R_K}^{\delta_2-2}\left((\delta_2-1)\left(b\alpha_1 G^{\alpha_2} K^{\alpha_1} - aK\varepsilon^{\beta}\right) + R_K w \delta_1\right)}{{D_1}^2 D_2 Y^3} \\
Y &= bK^{\alpha_1} G^{\alpha_2} - w(R_K + R_G) - a\varepsilon^{\beta} K
\end{aligned}
$$

and $D_1$ and $D_2$ being the first derivatives of the state dynamics with respect to the corresponding control

$$
\begin{aligned}
D_1 &= dK^{\delta_1}\delta_2 {R_K}^{\delta_2-1} \\
D_2 &= eG^{\sigma_1}\sigma_2 {R_G}^{\sigma_2-1}.
\end{aligned}
$$

In the boundary arc case, the optimal controls do not necessarily maximize the Hamiltonian, i.e. $\mathcal{H}_{R_K} = 0$ and $\mathcal{H}_{R_G} = 0$ might not be fulfilled in the optimum. Hence, the approach to derive the canonical system in the state-control-space, as done in (15a)-(19), cannot be used. Instead, the optimal controls have to maximize the Lagrangian. Therefore, in case of one or even both control constraints being active, the partial derivatives of the Lagrange function with respect to the controls, $\mathcal{L}_{R_K} = 0$ and $\mathcal{L}_{R_G} = 0$, together with the active constraint equations yield the corresponding Lagrange multipliers and the control dynamics, while the adjoint equations can be used to calculate the co-states. The state dynamics remain the same just with the according control values inserted, meaning $R_K = 0$ and/or $R_G = 0$. If, however, the mixed path constraint is fulfilled, the derivation of the according canonical system is more extensive. Assuming that the mixed path constraint is the only constraint being active, meaning that $R_K$ and $R_G$ are positive, the following DAEs have to be solved

$$
\begin{aligned}
\dot{K} &= A(K,G,R_K,R_G) \\
\dot{G} &= B(K,G,R_K,R_G) \\
\dot{\lambda_1} &= \lambda_1(r - A_K) - \frac{F_K(K,G) - \chi(\varepsilon)}{F(K,G) - w(R_K+R_G) - \chi(\varepsilon)K} - \mu_3(F_K(K,G) - \chi(\varepsilon)) \\
\dot{\lambda_2} &= \lambda_2(r - B_G) - \frac{F_G(K,G)}{F(K,G) - w(R_K+R_G) - \chi(\varepsilon)K} - \mu_3 F_G(K,G) \\
\mathcal{L}_{R_K} &= \mathcal{H}_{R_K} + \mu_3 C_{R_K} = 0 \\
\mathcal{L}_{R_G} &= \mathcal{H}_{R_G} + \mu_3 C_{R_G} = 0 \\
0 &= C(K,G,R_K,R_G)
\end{aligned}
$$

where $C$ defines the mixed path constraint and this time $\mu_3 \geq 0$. In order to transform these DAEs into

ordinary differential equations (ODEs), total time derivatives have to be considered:

$$\begin{aligned}
\frac{d}{dt}\mathcal{L}_{R_K} &= (\mathcal{H}_{R_KK}+\mu_3 C_{R_KK})\dot{K}+(\mathcal{H}_{R_KG}+\mu_3 C_{R_KG})\dot{G}+(\mathcal{H}_{R_KR_K}+\mu_3 C_{R_KR_K})\dot{R_K}+\\
&\quad (\mathcal{H}_{R_KR_G}+\mu_3 C_{R_KR_G})\dot{R_G}+\dot{\lambda_1}\mathcal{H}_{R_K\lambda_1}+\dot{\lambda_2}\mathcal{H}_{R_K\lambda_2}+\dot{\mu_3}C_{R_K}=0\\
\frac{d}{dt}\mathcal{L}_{R_G} &= (\mathcal{H}_{R_GK}+\mu_3 C_{R_GK})\dot{K}+(\mathcal{H}_{R_GG}+\mu_3 C_{R_GG})\dot{G}+(\mathcal{H}_{R_GR_K}+\mu_3 C_{R_GR_K})\dot{R_K}+\\
&\quad (\mathcal{H}_{R_GR_G}+\mu_3 C_{R_GR_G})\dot{R_G}+\dot{\lambda_1}\mathcal{H}_{R_G\lambda_1}+\dot{\lambda_2}\mathcal{H}_{R_G\lambda_2}+\dot{\mu_3}C_{R_G}=0\\
\frac{d}{dt}C &= C_K\dot{K}+C_G\dot{G}+C_{R_K}\dot{R_K}+C_{R_G}\dot{R_G}=0.
\end{aligned} \tag{20}$$

Inserting the according equations for $\dot{K}$,$\dot{G}$,$\dot{\lambda_1}$ and $\dot{\lambda_2}$ and solving the previous equations for $\dot{R_K}$,$\dot{R_G}$ and $\dot{\mu_3}$ yields the equations for the controls. Note, however, that $\dot{\lambda_1}$ and $\dot{\lambda_2}$ include $\lambda_1$ and $\lambda_2$ respectively, and therefore also $\dot{R_K}$, $\dot{R_G}$ are both dependent on the co-state. For this reason the reduction of the canonical system to four dimensions is not possible anymore and one has to consider all six dimensions which then are given as

$$\begin{aligned}
\dot{K} &= A(K,G,R_K,R_G) \\
\dot{G} &= B(K,G,R_K,R_G) \\
\dot{\lambda_1} &= r\lambda_1 - T_K - \lambda_1 A_K - \frac{T_{R_K}+\lambda_1 A_{R_K}}{w}(F_K-\chi(\varepsilon)) \\
\dot{\lambda_2} &= r\lambda_2 - T_G - \lambda_2 B_G - \frac{T_{R_G}+\lambda_2 B_{R_G}}{w}F_G \\
\dot{R_K} &= Y(K,G,R_K,R_G,\lambda_1,\lambda_2) \\
\dot{R_G} &= V(K,G,R_K,R_G,\lambda_1,\lambda_2)
\end{aligned} \tag{21}$$

where $T$ denotes the target function

$$T = \ln\left(F(K,G)-w(R_K+R_G)-\chi(\varepsilon)K\right)+u(\varepsilon)$$

and $Y$ and $V$ denote the obtained results for the control dynamics, which we omit here because they are very complex and don't allow any immediate insights.

### 3.2 Steady States

According to the maximum principle (see Grass et al. [2008]), in the following the maximization problem (6) subject to (6a)-(6k) will be solved by determining the stable manifolds arising from the canonical system which has been derived in the previous section. The steady states of the canonical system are determined by solving $\dot{K}=0$, $\dot{G}=0$, $\dot{R_K}=0$, $\dot{R_G}=0$ simultaneously. Considering the two state dynamics,

the according roots are obvious immediately:

$$\begin{aligned} K_{\dot{K}} &= \left(\frac{\phi}{dR_K{}^{\delta_2}}\right)^{\frac{1}{\delta_1-1}} \\ R_{K_{\dot{K}}} &= \left(\frac{\phi}{dK^{\delta_1-1}}\right)^{\frac{1}{\delta_2}} \\ G_{\dot{G}} &= \left(\frac{\psi}{eR_G{}^{\sigma_2}}\right)^{\frac{1}{\sigma_1-1}} \\ R_{G_{\dot{G}}} &= \left(\frac{\psi}{eG^{\sigma_1-1}}\right)^{\frac{1}{\sigma_2}} \end{aligned} \tag{22}$$

where subscripts denote the equation which is set to zero, respectively. Further on, also $K = 0$ and $G = 0$ would obviously be solutions. However, $K$ and $G$ occur in the denominator of $\dot{R_K}$ and $\dot{R_G}$ multiplicatively. Hence, for $K = G = 0$ we find no feasible steady state solution of the canonical system. Anyway, since the intention of environmental policy is not to let complete shut down of production be the only way to cope with introduced environmental standards, the main focus of this thesis lies on the determination of steady states with a positive production output. Inserting the roots in (22) together with parameter values into $\dot{R_K}$ and $\dot{R_G}$, the intersection of the isoclines $\dot{R_K} = 0$ and $\dot{R_G} = 0$ determines the steady states. In this first approach only one steady state can be detected, which will be demonstrated in what follows.

### 3.3 Stability

To determine the stability of this steady state, the Jacobian matrix is used, which is given by

$$J = \begin{pmatrix} \dot{K}_K & 0 & \dot{K}_{R_K} & 0 \\ 0 & \dot{G}_G & 0 & \dot{G}_{R_G} \\ \dot{R}_{K_K} & \dot{R}_{K_G} & \dot{R}_{K_{R_K}} & \dot{R}_{K_{R_G}} \\ \dot{R}_{G_K} & \dot{R}_{G_G} & \dot{R}_{G_{R_K}} & \dot{R}_{G_{R_G}} \end{pmatrix}, \tag{23}$$

where subscripts denote partial derivatives again. Hence the characteristic polynomial is

$$P(\mu) = \Big(\dot{K}_{R_K}\dot{R}_{K_K} - (\dot{K}_K - \mu)(\dot{R}_{K_{R_K}} - \mu)\Big)\Big(\dot{G}_{R_G}\dot{R}_{G_G} - (\dot{G}_G - \mu)(\dot{R}_{G_{R_G}} - \mu)\Big), \tag{24}$$

which determines four eigenvalues

$$\begin{aligned} \mu_{1,2} &= \frac{\dot{K}_K + \dot{R}_{K_{R_K}}}{2} \pm \underbrace{\sqrt{\frac{(\dot{K}_K - \dot{R}_{K_{R_K}})^2}{4} + \dot{K}_{R_K}\dot{R}_{K_K}}}_{X_1} \\ \mu_{3,4} &= \frac{\dot{G}_G + \dot{R}_{G_{R_G}}}{2} \pm \underbrace{\sqrt{\frac{(\dot{G}_G - \dot{R}_{G_{R_G}})^2}{4} + \dot{G}_{R_G}\dot{R}_{G_G}}}_{X_2}. \end{aligned} \tag{25}$$

Considering the sign of the determinant

$$\det J = \underbrace{(\dot{K}_{R_K}\dot{R}_{K_K} - \dot{K}_K\dot{R}_{K_{R_K}})}_{:=Z_1}\underbrace{(\dot{G}_{R_G}\dot{R}_{G_G} - \dot{G}_G\dot{R}_{G_{R_G}})}_{:=Z_2},$$

the cases summarized in Table 1 can be distinguished.

| det(J) | | Discriminant | Eigenvalues (EV) | Signs of real part of EV | Behavior |
|---|---|---|---|---|---|
| >0 | $Z_1, Z_2 > 0$ | $X_1, X_2 > 0$ | real with opposite signs | ( +,-,+,- ) | Saddle point |
| | $Z_1, Z_2 < 0$ | $X_1, X_2 > 0$ | real with same signs | ( -,-,+,+ ) | Saddle point |
| | | $X_1, X_2 < 0$ | complex | ( -,-,-,- ) | Stable |
| | | $sgn(X_1) \neq sgn(X_2)$ | real and complex | (+,+,+,+) | Repelling |
| <0 | $Z_1 > 0, Z_2 < 0$ | $X_1, X_2 > 0$ | real | (+,+,+,-) | Unstable |
| | | $X_1 < 0, X_2 > 0$ | real and complex | | |
| | $Z_1 < 0, Z_2 > 0$ | $X_1, X_2 > 0$ | real | ( -,-,-,+ ) | |
| | | $X_1 > 0, X_2 < 0$ | real and complex | | |

Table 1: Possible cases of stability.

### 3.4 The Laissez-Faire Scenario and the Introduction of Environmental Policy

At first, an economy is considered in which no environmental standards at all are imposed, i.e. $\varepsilon = 0$. In this laissez-faire scenario, the agent does not have to fulfill any environmental restrictions and therefore is completely free of abatement costs. However, this comes at the expense of environmental quality and consequently of the utility it yields. Anyway, as long as the utility of consumption is high enough to compensate for the loss of environmental quality, the agent's capital accumulation is somehow conceivable. Due to the fact that green capital is less productive than brown capital it is obvious that the agent will mainly use the polluting capital as much as possible. However, complete abandonment of green capital is not possible due to the assumption of a Cobb Douglas production function, but the green input factor is expected to be at least comparatively low. Figure 2 shows that the single steady state is at $K = 29,160$, $G = 4,126$ with control levels $R_K = 4,453$ and $R_G = 1,187$, which is a saddle point according to the first case in Table 1. Obviously $K$ is dominant in production. The colored region in Figure 2 corresponds to the admissible region according to the mixed path constraint $C \geq 0$.

In the next step, an economy with a medium environmental quality standard $\varepsilon = 0.4$ is considered. As one can see in Figure 3, this causes a big change in the position of the steady state. In this scenario, the saddle point is at $K = 714$, $G = 981$, $R_K = 24$ and $R_G = 96$. Due to the higher abatement cost, brown capital as dominant input factor has become too expensive. Green capital now is an essential substitute, despite its lower productivity. Comparing Figure 3 with Figure 2 one can see that the admissible region $C \geq 0$ shrinks with increasing $\varepsilon$.

Figure 4 finally shows the steady state for the basic model with constant returns to scale (CRS) in the production function, which is at $K = 904,808$, $G = 104,374$, $R_K = 545,908$ and $R_G = 333,154$. One can see that these equilibrium values are quite high, compared to the previous two scenarios. Also the admissible region expands with constant returns instead of decreasing returns to scale.

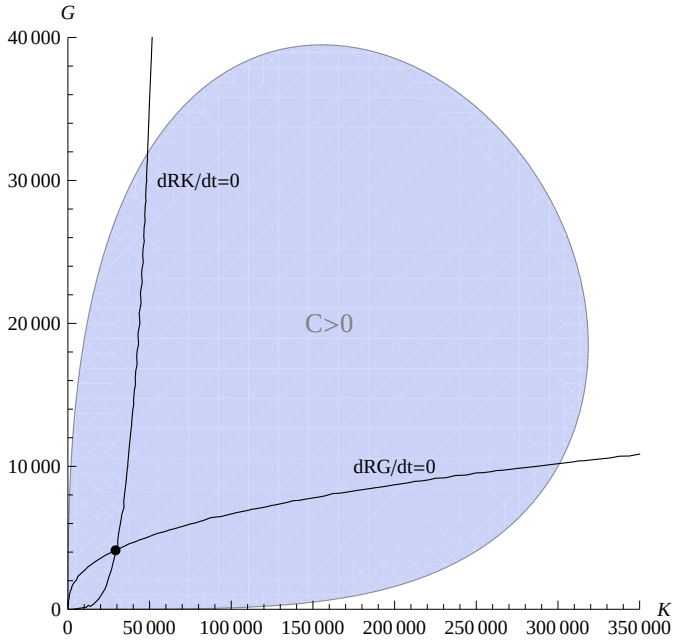


Figure 2: Steady state in the laissez-faire scencario for $\alpha_1 = 0.6$ and $\alpha_2 = 0.2$.

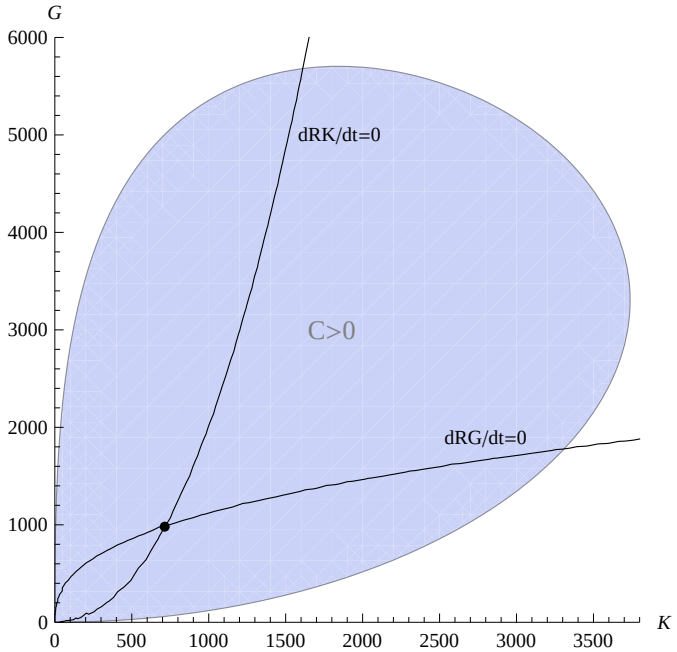


Figure 3: Steady state for $\alpha_1 = 0.6, \alpha_2 = 0.2$ and $\varepsilon = 0.4$.

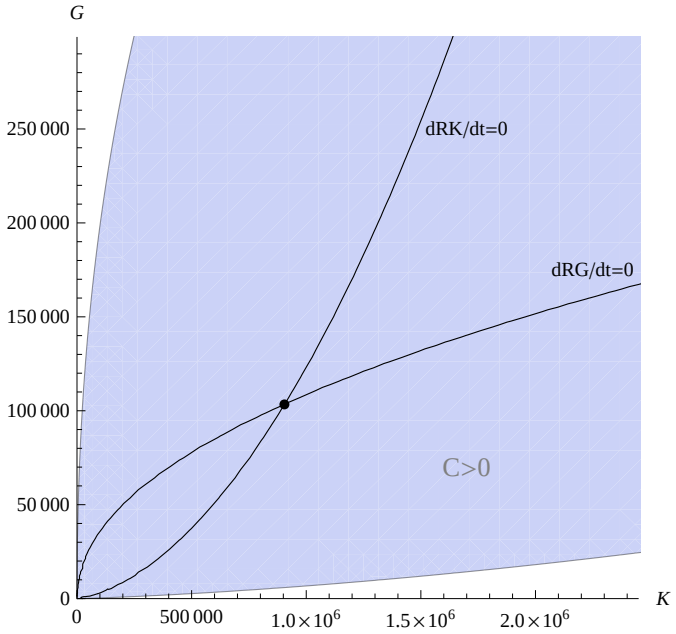


Figure 4: Steady state for CRS with $\alpha_1 = 0.7, \alpha_2 = 0.3$ and $\varepsilon = 0.4$.

# 4 Optimal Paths

In this section, the matter of interest is to find trajectories converging towards the equilibrium and to get the corresponding projections that cover a significant part of the $(K,G)$-plane. For this purpose, the initial value problem approach is used. Hence, initial values for a backward solution of the four-dimensional canonical system need to be constructed first. However, note that only the stable manifold leads directly into the equilibrium. Consequently, this set of starting points has to be very close to the equilibrium, in order to stay on or at least close to the stable manifold. Additionally, also dominant directions in the convergence to the steady state have to be considered. Therefore, an appropriate ellipse around the equilibrium is generated from which these starting points are taken. To take the dominant directions into account, the eigenvectors with negative eigenvalues are used for the calculation which is done by the formula

$$S = E + \frac{e_1}{|e_1|}\cos(\eta) + \frac{e_2}{|e_2|}\sin(\eta) \quad \text{with} \quad \eta \in [0, 2\pi], \tag{26}$$

where $S$ is the calculated starting point, $E$ denotes the equilibrium, and $e_1$ and $e_2$ are the corresponding eigenvectors. Within this calculation the values of the angle $\eta$ are close to $\frac{\pi}{2}$ and $\frac{3\pi}{2}$. This comes along with the fact that in those cases $\cos(\eta)$ is close to zero and therefore the dominant directions are weighted less here (cf. Knoll and Zuba [2004]). Based on these constructed initial values the canonical system is solved backwards. The projection of the resulting four-dimensional optimal trajectories onto the $(K,G)$-plane leads to a phase portrait, from which those trajectories have to be chosen, which correspond to the given initial conditions. In Figure 5 the phase portrait for $\varepsilon = 0.4$ is depicted. Here, the crucial and obviously very narrow intervals for the angle $\eta$ are $[0.4999755\pi, 0.4999756\pi]$ and $[1.500024418\pi, 1.500024419\pi]$.

As one can see in in Figure 5, some of the trajectories are divided into two parts. The first part, which is common for all and depicted in gray, corresponds to the backward solution of the system starting from

the equilibrium. On the left hand side the trajectories are continued until $K = 0$. On the right hand side, however, continuation aborts when the trajectories reach the boundary of the admissible region subject to the control constraint in (6c) where $R_K = 0$. This constraint is depicted in the figure as dashed black line. To enable further continuation of these trajectory paths, $R_K$ is constantly set to zero and calculation continues with the according canonical system where $\dot{R_K} = 0$. These second parts of the trajectories are depicted in black and their continuation is possible until they finally reach the admissible boundary of the mixed path constraint in (6e), where consumption, and therefore also utility from consumption, is zero.

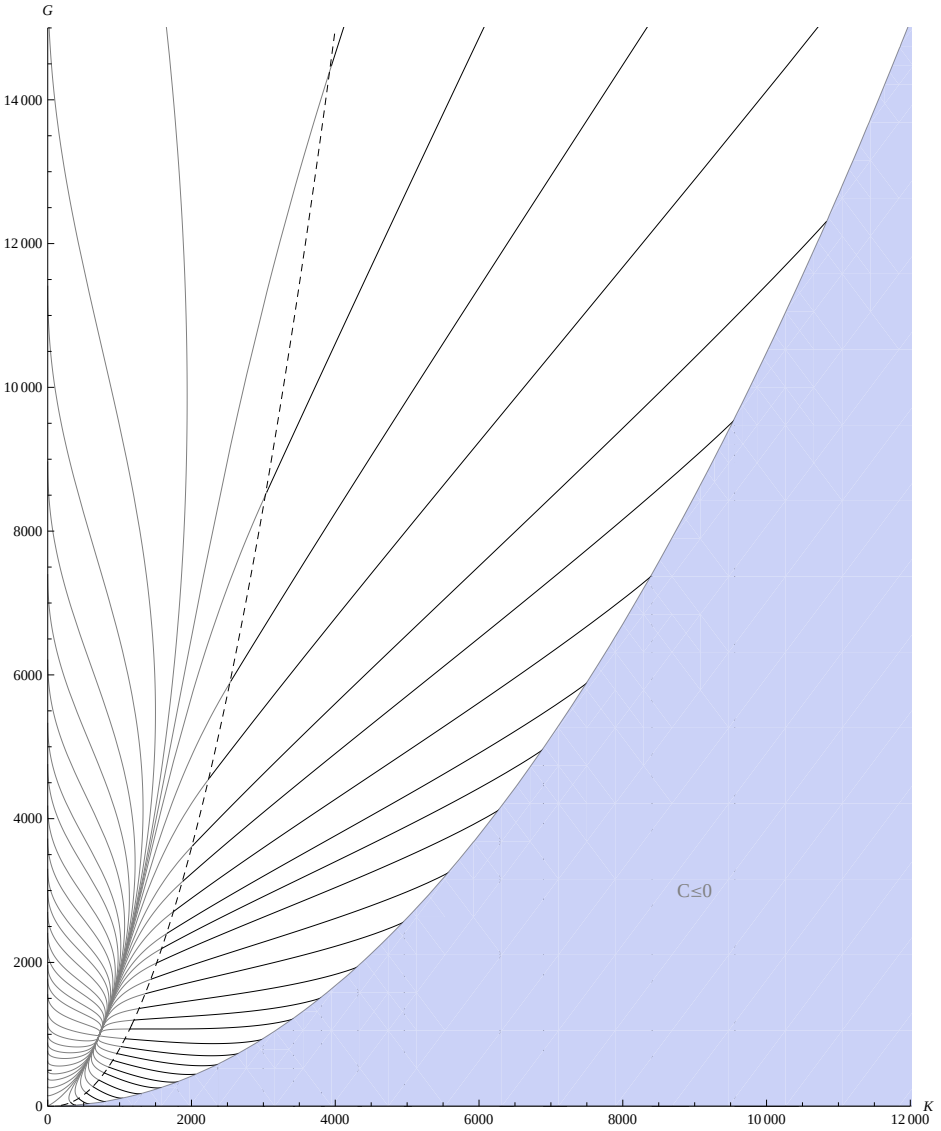


Figure 5: Phase portrait in $(K,G)$-space for $\alpha_1 = 0.6, \alpha_2 = 0.2$ and $\varepsilon = 0.4$.

## 4.1 Initial Points with an Equal Level of $K$ and $G$

Figure 6 shows two trajectories from the phase portrait in the ($K$,$G$)-plane which both have initial points with almost equal levels of $K$ and $G$. The first one starts at very low levels of brown and green capital which are smaller than the equilibrium values. Along the path to the equilibrium the levels of both types

of capital increase. The second trajectory has its initial point at a high level of brown and green capital above the equilibrium values. Accordingly, the levels of capital decrease along the trajectory while approaching the equilibrium.

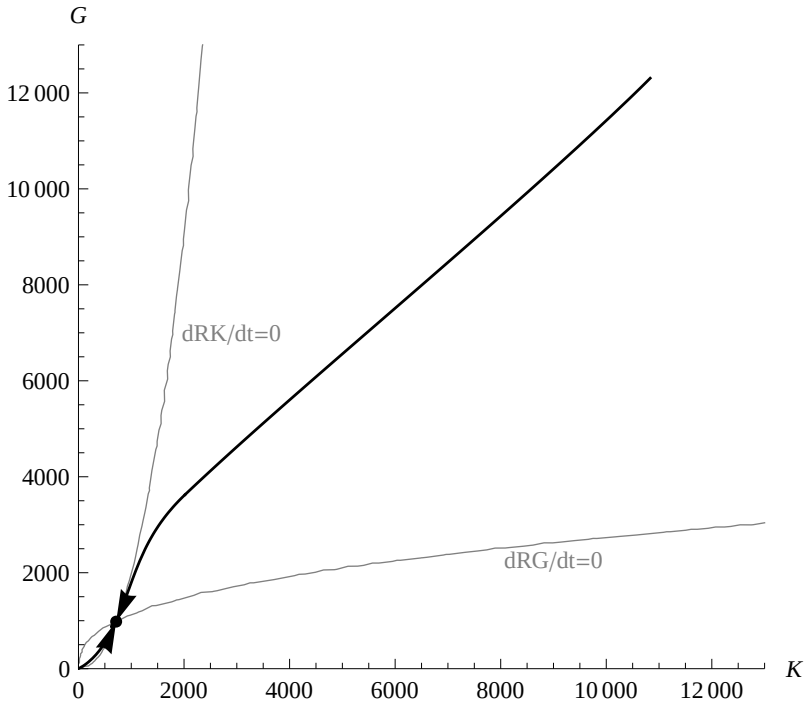


Figure 6: Two trajectories for $\alpha_1 = 0.6, \alpha_2 = 0.2$ and $\varepsilon = 0.4$ with equal initial capital levels.

Figure 7 shows the optimal time paths in $K$, $G$, $R_K$ and $R_G$ along the trajectory starting at the lower level of capital. As one can see, the levels of both types of capital increase monotonously while converging towards their equilibrium values, where conventional capital in the beginning is a little bit higher than green capital. Nevertheless, green capital finally gets dominant. Considering the paths of the R&D investments, the levels of $R_K$ and $R_G$ increase very quickly initially. Therefore less time is needed to get close to their equilibrium values. In order to cause growth in the capital levels, initially high R&D investments are needed until the positive feedback of the capital stock on itself is effective enough to thwart the negative pressure of depreciation. Note that the level of $R_K$ even decreases after reaching a peak to slow down this positive feedback until growth and depreciation are perfectly balanced close to the equilibrium. Due to the fact that the production elasticity of $R_G$ is less than the one of $R_K$, the behavior is different here. Higher investments are necessary to achieve the same effects and the $R_G$ level monotonously increases towards the equilibrium value.

In Figure 8 the same paths are considered for the trajectory starting at the high capital level. Here the levels of both capitals are decreasing. Due to the almost equal initial level of $K$ and $G$ and the comparatively lower equilibrium level of $K$, the decline of $K$ is stronger than in green capital. To switch off the positive feedback of $K$ on its own stock completely, and therefore to boost the negative impact of depreciation, $R_K$ initially is even zero and only rises again to stop this decline, but stays at a very low level, though. Due to lower production elasticity the level of green R&D initially rises very quickly up to a peak to stop the negative pressure of depreciation. Then it slightly decreases again to finally remain

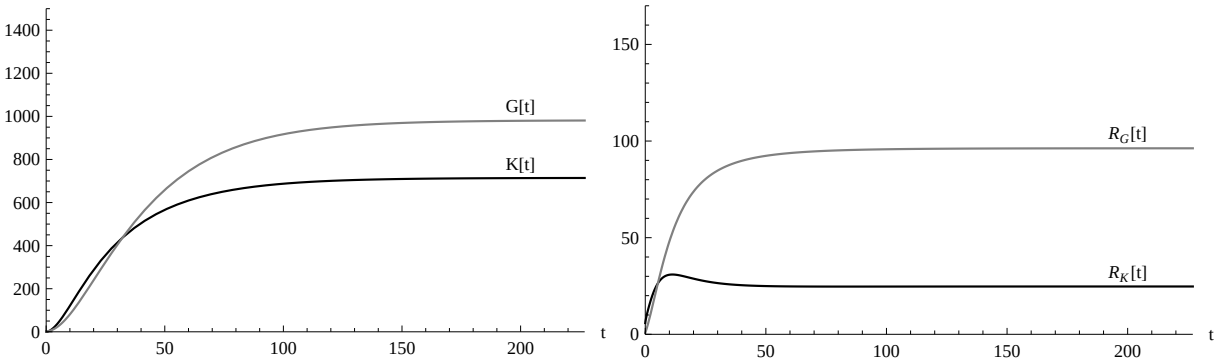


Figure 7: Optimal time paths of state and control starting from low capital levels for $\alpha_1 = 0.6, \alpha_2 = 0.2$ and $\varepsilon = 0.4$.

at a level obviously higher than the one of $R_K$.

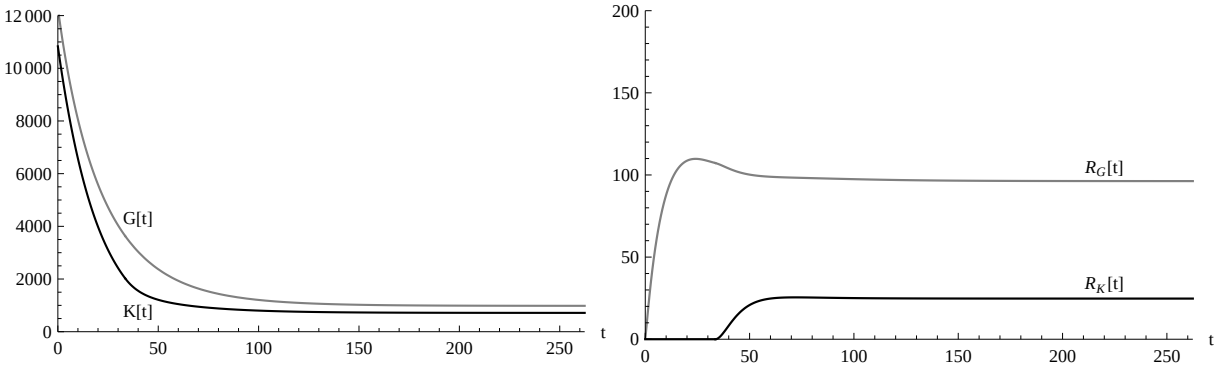


Figure 8: Optimal time paths of state and control starting from high capital levels for $\alpha_1 = 0.6, \alpha_2 = 0.2$ and $\varepsilon = 0.4$.

## 4.2 Initial Points with One Type of Capital Being Dominant

As mentioned above the initial use of both capital types is assumed due to the use of a Cobb Douglas production function. However, situations in which one type of capital is definitely the dominant input factor, whereas the other one almost equals zero, are certainly a matter of interest. Figure 9 shows two trajectories for such initial conditions. One either starts at a green capital-dominated production or in an initial point where $K$ is used almost exclusively as production input. In both cases, the level of the dominant capital lies above the equilibrium values, while the level of the dominated capital is below its equilibrium level.

Figure 10 shows the optimal time paths in the case of an initially green capital-dominated production. In contrast to the previous case of an almost balanced initial mix of production, the behavior of the capital levels in this dominated scenario are respectively opposed. Because green capital is dominant here, the level of $G$ decreases while brown capital, starting at a very low level, rises up to the equilibrium value. Considering the R&D investments, the same behavior as in Figure 7 can be observed, where $R_K$ rises up to a peak, then falls again and slows down the positive feedback, while $R_G$ increases monotonously.

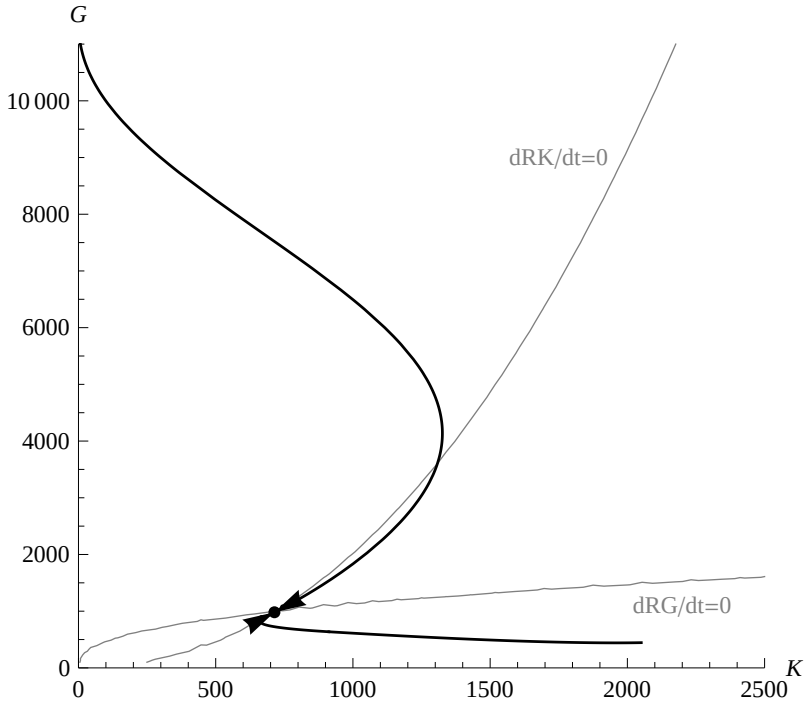


Figure 9: Two trajectories starting at a one-capital-type-dominated production for $\alpha_1 = 0.6, \alpha_2 = 0.2$ and $\varepsilon = 0.4$.

Summarizing this scenario it is interesting to see that $R_G$ is increasing while $G$ is decreasing. In other words, green R&D investments are made so to keep $G$ at a sufficiently high level.

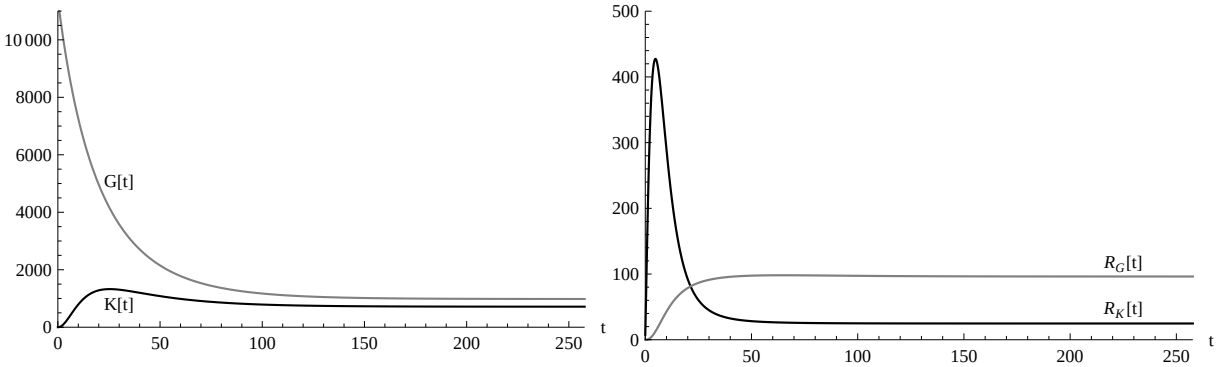


Figure 10: Optimal time paths of state and control starting from a definitely green capital-dominated production for $\alpha_1 = 0.6, \alpha_2 = 0.2$ and $\varepsilon = 0.4$.

Regarding the case of an initially brown capital-dominated production, the according optimal time paths are depicted in Figure 11. Accordingly, in this case $K$ decreases and $G$ rises up to the equilibrium values. Again, $R_K$ is initially zero and rises up to slow down the decline, while $R_G$ rises up to a peak and then slightly decreases.

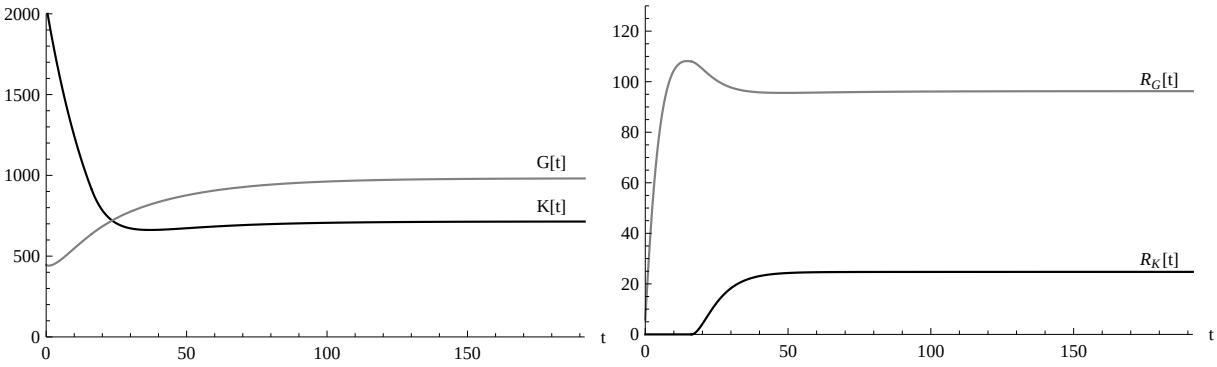


Figure 11: Optimal time paths of state and control starting from a definitely brown capital-dominated production for $\alpha_1 = 0.6, \alpha_2 = 0.2$ and $\varepsilon = 0.4$.

### 4.3 Bifurcation Analysis

In the previous sections, equilibria for specific values of $\varepsilon$ were considered. However, the main focus of this thesis is the investigation of the influence of the required environmental standards on the capital accumulation and hence on the production. In order to do this, bifurcation analysis is used with $\varepsilon$ being the varied parameter. Although only one steady state has been detected so far, and hence the bifurcation diagram for the basic model is quite simple, it gives a first idea about the interrelation of the environmental quality and the usage of both types of capital as input in production.

Figure 12 depicts the change of the equilibrium values under the variation of the environmental quality imposed by the government. For $\varepsilon = 0$ (laissez-faire scenario) $K$ is clearly dominant in production as already mentioned above. As one can see, increasing $\varepsilon$ results in an immediate decrease of $K$ due to the rising abatement cost per unit of brown capital. Also $G$ decreases with growing environmental quality. This might seem a little bit astonishing at first sight, but comes along with the fact that, due to the Cobb Douglas production function, a complete abandonment of $K$ as production input is impossible, and therefore a sufficiently small level of $K$ has to be used which at the same time has an increasingly absorbing impact on the productivity of $G$. However, this decrease is much smaller than the one of $K$. The point of special interest is at $\varepsilon = 0.362$. At this point, abatement gets so expensive that the use of green capital as dominant production input is more advantageous. In Figure 13 the changes of the equilibrium values of $R_K$ and $R_G$ over $\varepsilon$ are shown. They behave quite similarly. Initially, $R_K$ is dominant until abatement gets too expensive and higher investments in green R&D are optimal. This change happens already at $\varepsilon = 0.263$, i.e. earlier than for the capital stocks.

Note, however, that in this basic model increasing environmental standards in general have a diminishing impact on the production inputs, and therefore on production output, and furthermore on economic growth. As one can see in Figure 14, the production is strictly monotonously decreasing.

In contrast, the utility function as depicted in Figure 15 rises up to a peak before it decreases due to the trade-off between consumption and environmental quality. If $\varepsilon$ is small enough, a small loss in consumption in return for a slightly better environment is advantageous. The utility-maximizing environmental quality is at $\varepsilon = 0.125$.

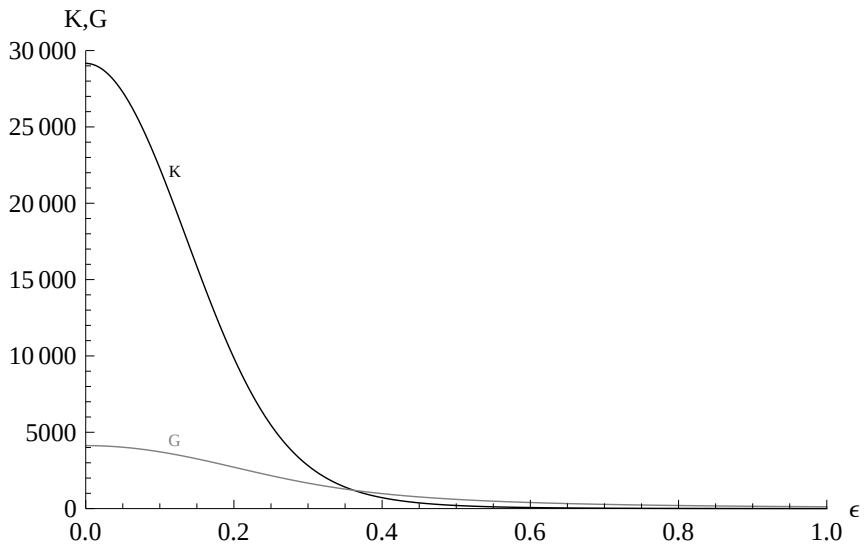


Figure 12: Bifurcation diagram for steady state levels of $K$ and $G$ with respect to $\varepsilon$ for $\alpha_1 = 0.6$, $\alpha_2 = 0.2$.

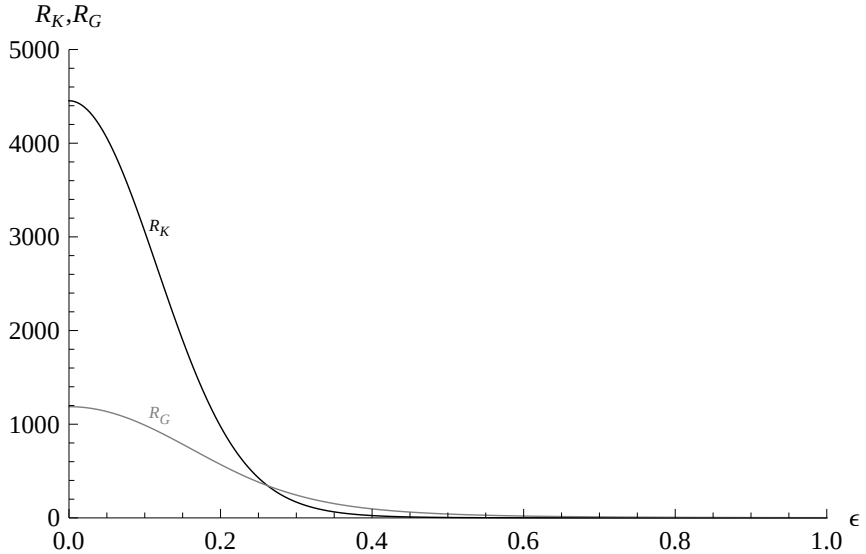


Figure 13: Bifurcation diagram for steady state levels of $R_K$ and $R_G$ with respect to $\varepsilon$ for $\alpha_1 = 0.6$, $\alpha_2 = 0.2$.

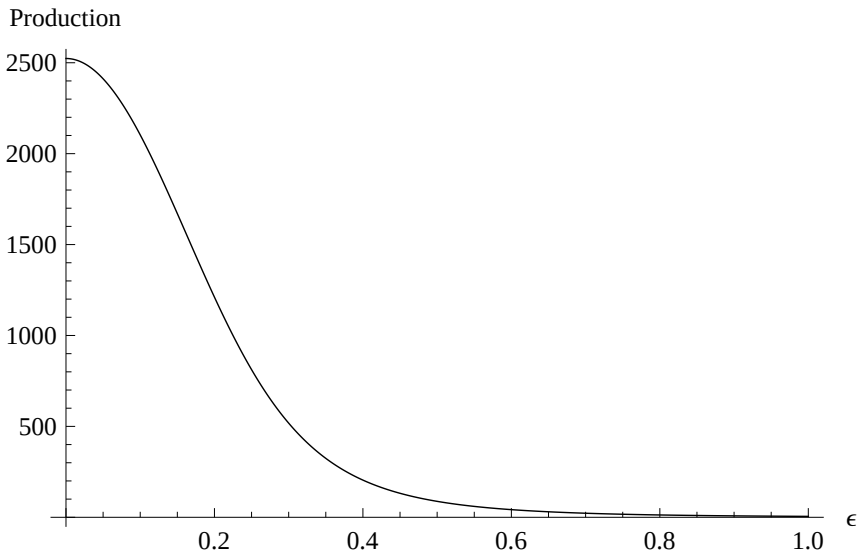


Figure 14: Bifurcation diagram of the steady state production output with respect to $\varepsilon$ for $\alpha_1 = 0.6$, $\alpha_2 = 0.2$.

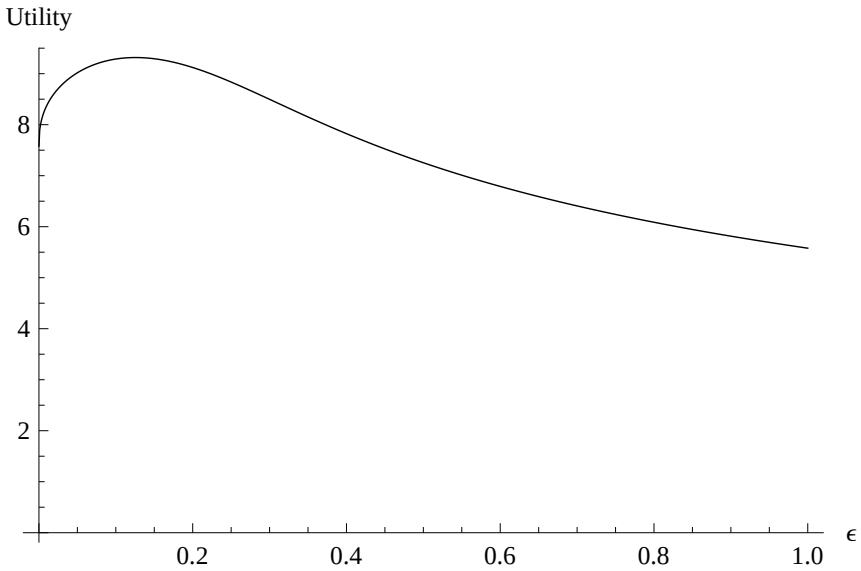


Figure 15: Bifurcation diagram of equilibrium utility with respect to $\varepsilon$ for $\alpha_1 = 0.6$, $\alpha_2 = 0.2$.

In order to get a more qualitative than a quantitative comparison of the changing usage of $K$ and $G$ with increasing $\varepsilon$, the ratios of both are shown in Figure 16. As one can see, the ratio of $G$ follows a convex-concave shape. At the beginning, the usage of $G$ is quite low and does not change much with increasing $\varepsilon$. In this area, the abatement costs are still too low to change the advantage of conventional capital. The inflexion point is at $\varepsilon = 0.362$ where green capital starts to dominate conventional capital. From here on the ratio of $G$ grows quite quickly until it converges to almost 100%. Note however, that 100% can never be reached. Accordingly, the ratio of $K$ follows a concave-convex decrease.

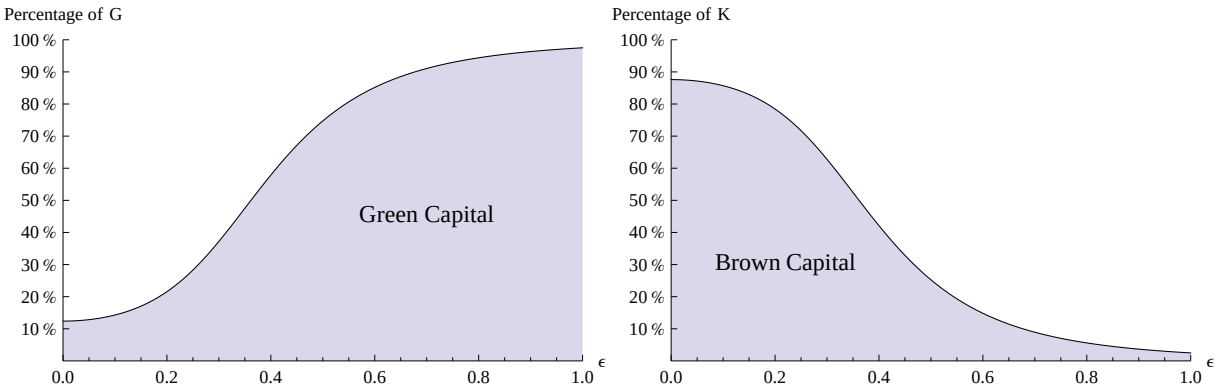


Figure 16: Bifurcation diagram of the equilibrium ratios of $K$ and $G$ with respect to $\varepsilon$ for $\alpha_1 = 0.6$, $\alpha_2 = 0.2$.

In Figure 17 the ratios of the according R&D investments are depicted. Their development is similar, the only difference is the position of the inflexion point which is already at $\varepsilon = 0.263$.

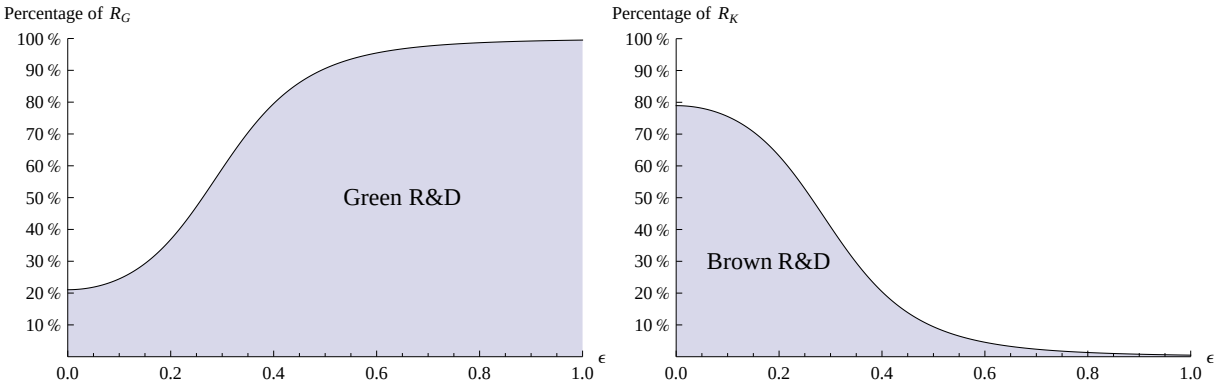


Figure 17: Bifurcation diagram of the equilibrium ratios of $R_K$ and $R_G$ with respect to $\varepsilon$ for $\alpha_1 = 0.6$, $\alpha_2 = 0.2$.

# 5 Conclusion

The aim of this work is to investigate how environmental regulation influences economic growth as well as R&D investments and whether or not they induce a shift to a greener technology.

As far as economic growth is concerned, it becomes obvious that increasing stringency of environmental regulation causes a decline in both types of capital and consequently also in production output. Therefore it rather represses than supports economic growth.

However, the carried out analysis shows, that increasing environmental regulation indeed has a positive impact on the accumulation of green capital and on the increase of green R&D investments. This can especially be seen when the shares of capital levels and R&D investments under varying stringency of environmental standards are considered. Although both capital levels decline, increasing abatement costs even accelerate the decrease of brown capital levels so that in total production turns out to be greener the higher environmental quality standards are. Same applies for R&D investments.

To sum up, environmental regulation standards can cause a shift to greener production but only at the cost of repressed economic growth. Therefore, the introduction of additional environmental instruments, such as taxes or maybe subsidies, might be interesting and could possibly be helpful to archive better results. Moreover, also the usage of a pollution function describing the environmental condition will be matter of future work.

# References


D. Grass, J.P. Caulkins, G. Feichtinger, G. Tragler, and D.A. Behrens. *Optimal Control of Nonlinear Processes - With Applications in Drugs, Corruption and Terror*. Springer, Heidelberg, 2008.

IPCC. *Climate Change 2007*. International Panel on Climate Change, 2007.

C. Knoll and D.M. Zuba. *Dynamic Models of the US Cocaine Epidemic: Modeling Initiation and Demand and Computing Optimal Controls*. PhD thesis, TU Wien, May 2004.

M. Rauscher. Green R&D versus end-of-pipe emission abatement: A model of directed technical change. *Thuenen-Series of Applied Economic Theory*, 106, 2009.

K. Richardson et al. *Synthesis Report from Climate Change: Global Risks, Challenges and Decisions.* University of Copenhagen, 2009.

# Appendix

| Parameter | Value | Description |
|---|---|---|
| $a$ | 1 | Constant of proportionality of abatement costs |
| $b$ | 1 | Scale parameter of the production function |
| $c$ | 5 | Scale parameter describing the utility of environmental quality |
| $d$ | 1 | Scale parameter of $\dot{K}$ |
| $e$ | 1 | Scale parameter of $\dot{G}$ |
| $r$ | 0.05 | Discount rate |
| $w$ | 0.1 | Opportunity cost of research |
| $\beta$ | 2 | Exponent of abatement costs |
| $\gamma$ | 0.4 | Exponent describing the utility of environmental quality |
| $\delta_1$ | 0.3 | Production elasticity of $K$ in $\dot{K}$ |
| $\delta_2$ | 0.5 | Production elasticity of $R_K$ in $\dot{K}$ |
| $\sigma_1$ | 0.3 | Production elasticity of $G$ in $\dot{G}$ |
| $\sigma_2$ | 0.4 | Production elasticity of $R_G$ in $\dot{G}$ |
| $\phi$ | 0.05 | Depreciation rate of $\dot{K}$ |
| $\psi$ | 0.05 | Depreciation rate of $\dot{G}$ |

Table 2: Parameter values.